Analysis of Water Cluster Structures and Mass Transport in Polymer Electrolyte Membranes Containing Cerium Ions Using Molecular Dynamics Simulations

Kyohei Ishikawa[*1,2], Takuya Mabuchi[*2,3], Takashi Tokumasu[*2]

[*1]Graduate School of Engineering, Tohoku University,

[*2]Institute of Fluid Science, Tohoku University,

[*3]The Frontier Research Institute for Interdiscipliary Sciences, Tohoku University

Abstract：We analyzed the effect of cerium ions, which are added to improve the chemical durability of a polymer electrolyte membrane（PEM）, on the membrane structure and proton transport properties using molecular dynamics simulations. We found that at low water content the water cluster connectivity is enhanced by the addition of a small amount of cerium ions（0.6-1.8 wt%）that attract the surrounding water molecules. Hence, better proton diffusion pathways are formed, leading to an increase in the proton diffusion coefficient. At high water content, however, because the water clusters are well connected, regardless of the cerium ion content in the PEM, the presence of cerium ions hinders proton transport, resulting in a decrease in the proton diffusion coefficient.

Key Words：Polymer electrolyte fuel cell, Molecular dynamics, Proton transport, Cerium ion, Durability.

1． Introduction

Polymer electrolyte fuel cells（PEFCs）are highly regarded as a promising technology for stationary power generation and automobiles. To expand the wider use of PEFCs, improvements in the power density of unit cells are necessary[1]. Proton transport in the membrane electrode assembly（MEA）is closely associated with achieving improved power density. Hence, clarifying the correlation between the structure of the membrane and proton transport at the molecular level is important. In particular, when considering proton conductivity, it is the polymer electrolyte membranes（PEMs）that require optimization[2]. A perfluorosulfonic acid membrane having a sulfonic acid group（-SO$_3$H）, such as Nafion, Flemion, or Aciplex, is mainly used as a PEM. In PEMs, high proton conductivity is required to improve the power generation efficiency. Protons are transported in a PEM by two different mechanisms: i.e., vehicle and Grotthuss mechanisms. A proton typically exists as a hydronium ion, which is the smallest stable hydrated form of an excess proton in water, upon combination with a water molecule. In the vehicle mechanism, protons are transported

by the molecular motion of hydronium ions. In the Grotthuss mechanism, protons move by the connecting and disconnecting of the O-H bond between the hydronium ion and the water molecule. Protons diffuse much faster by the Grotthuss mechanism than by the vehicle mechanism, but the effect of Grotthuss mechanism on proton conductivity is reduced without an abundance of water molecules around the hydronium ions. The proton transport properties in a PEM are greatly influenced by the structure of the water clusters[3]-[6]. One of the factors affecting the structure of a water cluster is the water content of the PEM. Experimental and computational studies have reported that an increase in the water content leads to improvement in the connectivity of clusters and an increase in the diffusivity of protons in a PEM due to the increased diffusivity by both transport mechanisms.

An improvement in the durability of PEFCs is clearly required, therefore, it is important to clarify the causes of deterioration and take the necessary remedial action[7]. Chemical degradation of PEMs is considered to be one of the causes of deterioration[8]. An hydroxyl radical（OH·）is generated by the decomposition of hydrogen perox-

ide, generated by an oxygen reduction reaction during PEFC operation. This OH has high reactivity and it will degrade the polymer membrane[9)-11)]. Based on this degradation mechanism, the method of adding a substance that inactivates OHs before they react with the polymer (i.e., a radical scavenger) has been put into practical use. One of the most useful radical scavengers is the cerium ion[12)-14)]. However, previous studies have reported that cerium ions in a PEM migrate during operation and the distribution becomes nonuniform. At points where there are only a few cerium ions in the membrane, the effect as a radical scavenger is lost and degradation occurs[15), 16)]. Therefore, it is important to elucidate the transport mechanism of the cerium ion in a PEM. Furthermore, the cerium ion is a trivalent ion, hence its large charge probably affects proton transport and water distribution in the membrane[17)]. It is very difficult to investigate the structure in a PEM experimentally and the mechanism that determines the relationship between structure and transport in a PEM has not yet been elucidated. Therefore, analysis by numerical simulation is considered effective.

Mabuchi and Tokumasu used molecular dynamics (MD) simulations to analyze proton transport properties in a Nafion bulk membrane and elucidated the relationship between the cluster structure and the contributions of the vehicle mechanism and the Grotthuss mechanism in electro-osmosis and proton transport[4), 6)]. Kawai et al. used MD simulations to analyze the structure and proton transport in a Nafion bulk membrane containing ferrous ions and elucidated that clusters will bind and proton diffusivity probably improve when a certain amount of ferrous ions is added at low water contents[17)]. Endoh et al. experimentally clarified the increase in durability of a membrane upon the addition of cerium ions under low temperature and low humidity conditions[14)]. Wong et al. developed a comprehensive chemical decomposition model for the ceria-added MEA. They indicated that the cerium ions will be transported to the cathode catalyst layer side at low cell voltages and the degradation rate of the membrane probably increases[18)]. However, molecular analysis of water cluster structure and mass transport of PEMs containing cerium ions is insufficient. In this study, we modeled PEMs containing cerium ions using MD simulations and analyzed the effects of chang-

es in water content and cerium ion addition on the water structure, ion distribution, and mass transport properties in the membrane.

2．Simulation methods

We constructed a Nafion bulk membrane system containing cerium ions and analyzed the effects of the water content and cerium ion addition rate (CAR) on the structure, molecular distribution, and mass transport properties of the membrane using MD simulation. Fig. 1 shows the chemical structure of Nafion model with the equivalent weight of 1146 used in the present study. The all-atom DREIDING force field was adopted for the molecular interaction of Nafion,[19)] and the particle mesh Ewald method was used to calculate the Coulomb force.[20)]
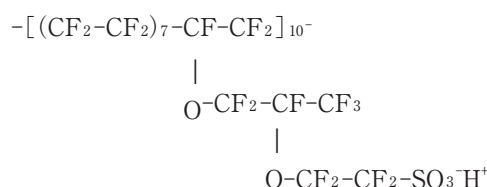
$$-[(CF_2-CF_2)_7-CF-CF_2]_{10}-$$
$$|$$
$$O-CF_2-CF-CF_3$$
$$|$$
$$O-CF_2-CF_2-SO_3^-H^+$$

Fig. 1　Chemical structure of the Nafion polymer.

The cutoff distance of the Lennard-Jones and Coulomb potentials was set at $r_c = 12$ Å. The anharmonic two-state empirical valence bond (aTS-EVB) model was used for water molecules and hydronium ions[21)]. Using this model, we can perform simulations incorporating the Grotthuss mechanism (one of the proton conduction mechanisms, mentioned earlier). The positive charge of the hydronium ion and the cerium ion was balanced with the negative charge of the sulfonic acid group in the system. The number of water molecules was determined by the water content, λ, as shown in equation (1),

$$\lambda = (N_{H2O}+N_{H3O+}) / N_{SO3-}, \qquad (1)$$

where N_{H2O}, N_{H3O+}, and N_{SO3-} represent the numbers of each of the molecules. The water content was set at $\lambda = 3, 6, 9$, and 12, which correspond to the water content in the bulk Nafion membrane at approximately RH = 20%, 60%, 80%, and 85%, respectively[22)]. The CAR was determined to correspond to 0-15% of the total number of sulfonic acid groups in the membrane. Three-dimensional periodic boundary conditions were applied to the

simulation system. This simulation system is shown in Fig.2 The construction procedure of the simulation system is as follows. First, Nafion chains, water molecules, hydronium ions, and cerium ions were randomly placed in a simulation system (x × y × z = 200 × 200 × 200 $Å^3$).
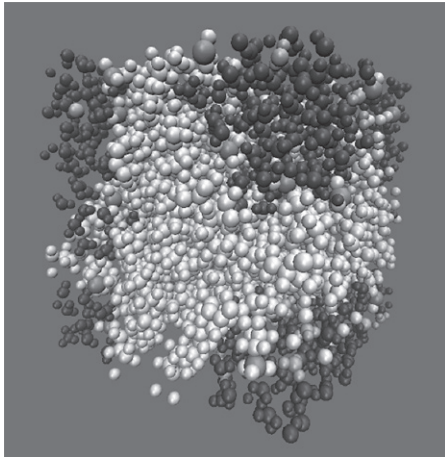

Fig. 2 Snapshot of the simulation system：$λ$ = 12 and CAR. = 10%. (White beads: Nafion, red beads：sulfur, green beads：cerium ions, blue beads：water, orange beads: hydronium ions.)

Table 1 shows the number of molecules in the system. Next, annealing was performed. Temperature was controlled by the Nosé-Hoover method[23] and pressure was controlled by the Andersen method[24].

Table 1　Number of molecules in the calculation system.

Water content $λ$	Nafion	Ce^{3+}	H_2O	H_3O^+
3	4	0-6	80-98	22-40
6	4	0-6	200-218	22-40
9	4	0-6	320-338	22-40
12	4	0-6	440-458	22-40

The annealing procedure was as follows (where the following abbreviations apply: N is the number of molecules, V is the volume of the system, T is the temperature of the system, and P is the pressure of the system):
［1］Simulation system was compressed by the NPT ensemble at 350 K and 1 MPa for 190 ps.
［2］NVT ensemble at 800 K for 40 ps.
［3］NPT ensemble at 350 K and 0.1 MPa for 40 ps.
［4］Step［2］and step［3］were repeated five times. Since the densities of the system were almost the same after the fourth and fifth steps, the system

was judged to have reached the most stable state.
［5］NPT ensemble at 350 K and 0.1 MPa for 100 ps.
［6］NVT ensemble at 350 K for 1500 ps.

After annealing, the production run was performed for 24 ns using the NVT ensemble. The time step was set at 1 fs and the sampling interval was 10,000 steps. The simulation was performed once under each condition, and two times additional simulations were performed for the $λ$ = 3 with different diffusion coefficient trends. The temperature and density applied during the annealing process are shown in Fig.3 In the fourth and fifth NPT ensembles of Step 4, to reach equilibrium state the system was judged because there was almost no change in density.
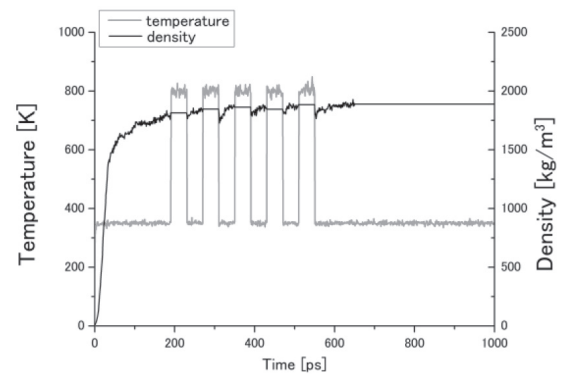

Fig. 3　Relaxation process for annealing.

3．Result and discussion

3．1　Diffusion coefficient

The self-diffusion coefficient was calculated from the mean square displacement (MSD) using Einstein's equation (2),

$$D = \lim_{t \to \infty} \frac{1}{6(t-t_0)} \left\langle \left| r(t) - r(t_0) \right|^2 \right\rangle , \tag{2}$$

where $\langle\ \rangle$ is the time average, t is the diffusion time, r is the atomic position vector, and D is the self-diffusion coefficient. The self-diffusion coefficient was calculated from the liner regime of MSD curves from 0.2 to 0.3 ns. The self-diffusion coefficient was converted to the membrane resistance and compared with the experimental value[15]. The conductivity was obtained using the Nernst-Einstein equation (3) and converted into a membrane resistance using equation (4),

$$\sigma = \frac{e^2 nD}{k_B T} \quad , \tag{3}$$

$$R = \frac{1}{\sigma} \quad , \tag{4}$$

where e is the elementary charge, n is the number density, k_B is the Boltzmann constant, and T is the temperature. Fig.4 and Fig.5 show the proton diffusion coefficient and membrane resistance, respectively. The diffusion coefficient value at CAR = 0% and the decrease in proton conductivity with increasing CAR at high water content are well consistent with previous experimental researches[22), 25)]. Therefore, we believe that the simulated system reproduces reasonable physical properties. The diffusion coefficient increases with increasing water content regardless of the CAR. The membrane resistance tends to increase as the CAR increases due to a decrease in the diffusion coefficient of protons or a decrease in the proton concentration in the membrane[15)]. In particu-
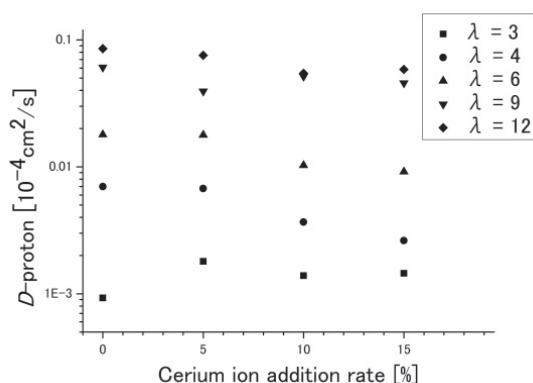
lar, a decrease in the diffusion coefficient is dominant, compared to the decrease in the proton concentration, at low water content. However, at $\lambda = 3$ and CAR = 5, 10%, the increase in the membrane resistance is reduced because the diffusion coefficient of proton increases, compared with when no cerium is added. Therefore, in the next section (3.2), we will compare the structures when $\lambda = 3$ and $\lambda = 12$, and consider the causes of the increase in diffusivity.

Fig.6 shows the self-diffusion coefficient of cerium ion. The diffusion coefficient increases with increasing water content. This is in agreement with experimental results[26)]. There was no clear relationship between the CAR and the diffusion coefficient. The mass transport characteristics described above are probably greatly affected by a change in the membrane structure, upon an increase in water content; therefore, in the next section (3.2), we will discuss these reasons, based on structural analysis.
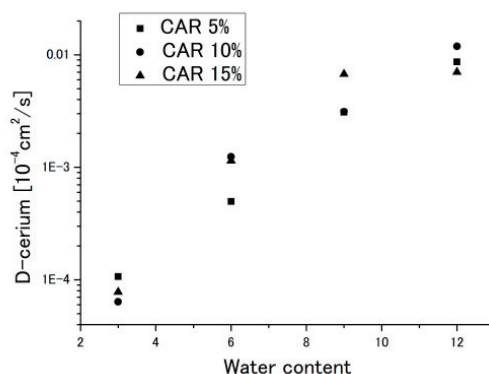

Fig.4　Self-diffusion coefficient of protons.

Fig.5　Membrane resistance at various water contents.

Fig.6　Self-diffusion coefficient of cerium ions.

3.2　Structural analysis

The dependence of the molecular structure in a PEM on the water content and the CAR was analyzed using the radial distribution function (RDF). Because the membrane resistance, depending on the presence or absence of cerium ions, differs between at low water content and at high water content, the analysis was performed focusing on the structural change inside the PEM with an increase in the water content. Fig.7 shows the RDF $g_{S\text{-}Ce}(r)$ between the sulfonic acid group and the cerium ion with an increase in the water content when the CAR = 10%. The first peak emerges at $r = 4.1$ Å, the height of which decreases as the water content increases. There-

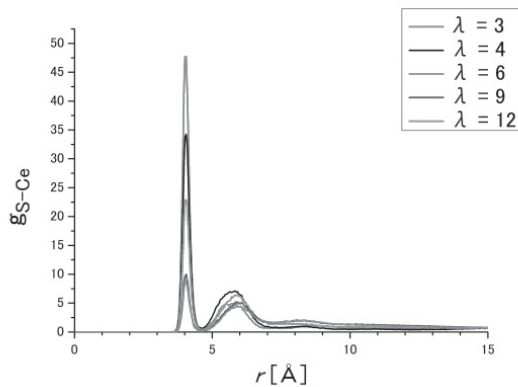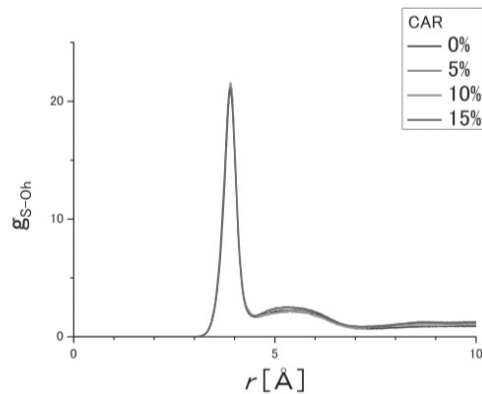Fig. 7　RDF of sulfur-cerium ion（CAR 10%）.

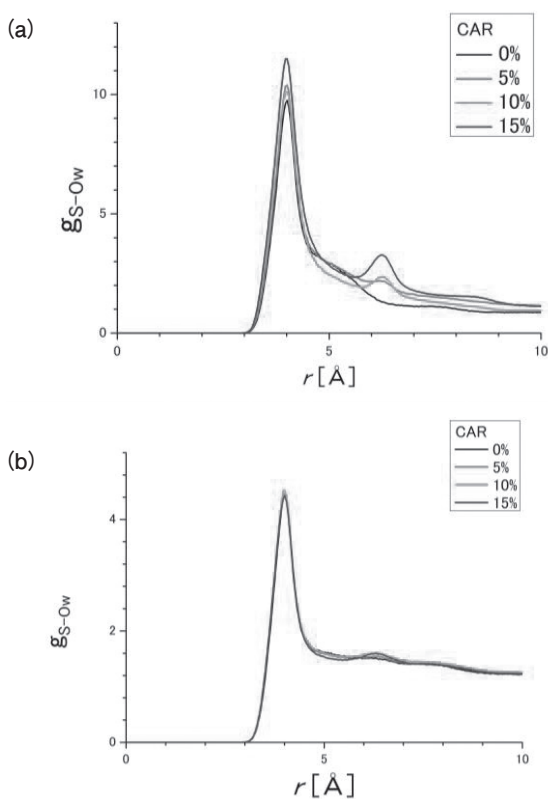Fig. 9　RDF of sulfur-hydronium oxygen（λ = 3）.

(a)

(b)

Fig. 8　RDF of sulfur-water oxygen:
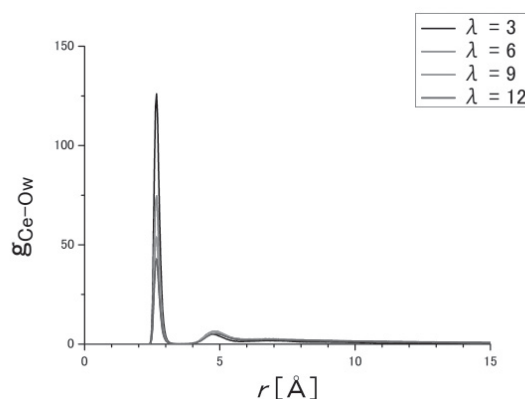　　　　(a) when λ = 3 and (b) when λ = 12.

Fig. 10　RDF of cerium ion-water oxygen（CAR 10%）.

fore, the indications are that the distribution of cerium ions in the membrane is concentrated around the sulfonic acid group and spread out into the solvent, away from the sulfonic acid group, as the number of water molecules increases. This also occurs, even when there is a change in the CAR.

　Fig. 8（a）,（b）shows the RDF $g_{S-Ow}(r)$ between the sulfonic acid group and the water molecules when λ = 3 and λ = 12. Fig. 9 shows the RDF $g_{S-Oh}(r)$ between the

sulfonic acid group and the hydronium ions when λ = 3. The first peak is observed at r = 4.1 Å in both the water molecule and the hydronium ion, indicating that these are concentrated around the sulfonic acid group as well as the distribution of cerium ion. In addition, the second peaks appear at r = 6.2 Å in the 8（a）,（b）due to the addition of cerium ions. This indicates that the cerium ions that are around the sulfonic acid groups attract water molecules, hence the water distribution changes. The second peak is more apparent because the water content is lower. From the above, we observed that cerium ions, water molecules, and hydronium ions exist around the sulfonic acid group, and at low water content, more water molecules are attracted by the addition of the cerium ions. This is probably related to the decrease in membrane resistance at low water content due to the small amount of cerium addition（described in the previous section）because the cerium ions would bind water clusters. This point will be examined in the later cluster analysis（see Section 3.3）.

Fig.10 shows the RDF $g_{Ce-Ow}(r)$ between the cerium ion and the water molecules with an increase in the water content when CAR = 10%. There is a peak at $r = 2.7$ Å, and the position of the peak does not change with the water content. Figs 11 and 12 show the coordination numbers of cerium ions to sulfonic acid groups and water molecules to cerium ions, respectively. As the water content increases, the coordination number of the cerium ion around the sulfonic acid group decreases, and the coordination number of water molecules around the cerium ion increases. Furthermore, the coordination number of water molecules around the cerium ion is sufficiently large (5.5-8.2), regardless of the water content. This implies that there are normally many water molecules around the cerium ion, indicating that the cerium ion exists inside the water cluster. From the above, we considered that the cerium ions are concentrated around the sulfonic acid group at low water content but as the water content increases the cerium ions move away from the sulfonic acid group into the water cluster and
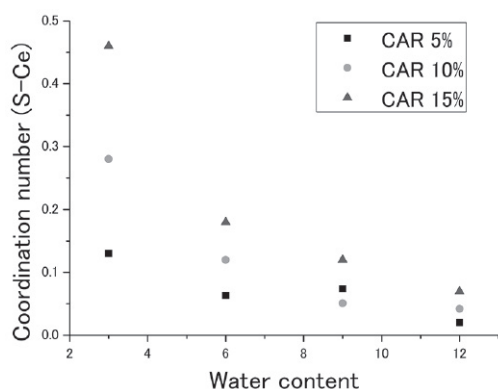
are distributed throughout the whole membrane. This change in the distribution of cerium ions is thought to be related to the increase in the diffusion coefficient of cerium ions with increasing water content.

3.3 Cluster analysis

Next, we analyzed the number of clusters and the cluster size. In this calculation, a water cluster is defined as a water and hydronium ion aggregate in which the intermolecular distance of the oxygen atom of the water molecule is within 3.4 Å. This distance of 3.4 Å is the terminal value of the first peak in the RDF between oxygen atoms of water molecules in the Nafion bulk membrane (see Fig.13). This value is consistent with the value used for cluster analysis in the previous study.[6] In this study, the number of water molecules contained in a cluster is defined as the cluster size.

Fig.14 shows the average number of clusters of each CAR value at λ = 3 and 12 and Fig.15 shows the average cluster size of each CAR value at λ = 3 and 12. At λ = 3, the number of clusters decreases and the average cluster size increases with an increase in CAR. At λ = 12, however, no significant change was observed in the number of clusters and the average cluster size at each CAR. Furthermore, upon comparing the results according to water content, we observed that the number of clusters decreases and the average cluster size increases as the water content increases.

From the above, we deduced that the cerium ions gather around the surrounding water molecules by electric charges and bind clusters at low water content, as shown in Fig.16 (a). At low water content, CAR = 15%,
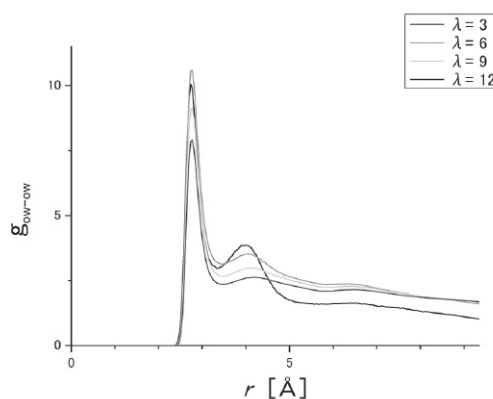

Fig.11　Coordination number of cerium ions around sulfonic groups.
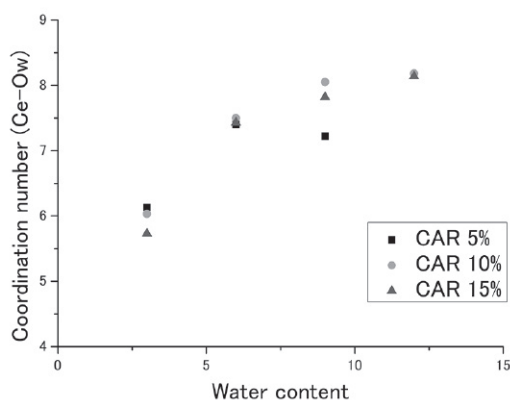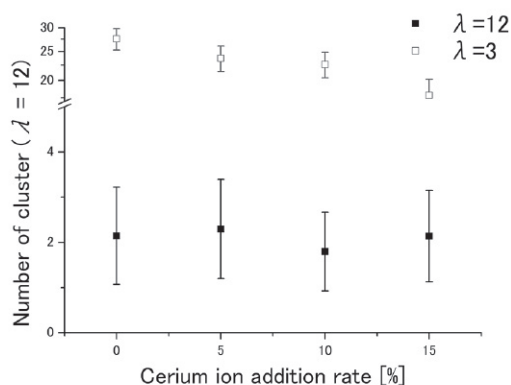

Fig.12　Coordination number of water oxygens around cerium ions.

Fig.13　RDF of water oxygen-water oxygen.

Fig.14　Number of clusters at λ = 3 and 12.

Fig. 15 Average cluster size at λ = 3 and 12.

Fig.16　Schematic of the structure of the sulfonic groups and water clusters： (a) when λ = 3 and (b) when λ = 12.
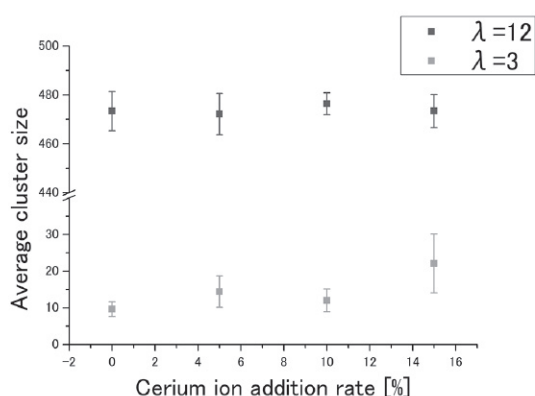
the connectivity of clusters is enhanced, but the proton diffusivity is considered to have decreased because the increase of Ce ion concentration increases the hindrance of proton transport by the electric charge of Ce ion. Then, because the clusters have already connected sufficiently at high water content (Fig.16 (b)), we considered that the cerium ion has almost no effect on the cluster structure.

4．Conclusion

In this study, we analyzed in the effects of the cerium ion addition rate and the water content on the proton and cerium ion transport properties and the structural properties in a PEM using MD simulations that takes into account the Grotthuss mechanism.

At low water content, upon the addition of a small amount of cerium ions in the membrane, an improvement in the proton diffusion coefficient was found. The cerium ions around the sulfonic acid group attract sur-
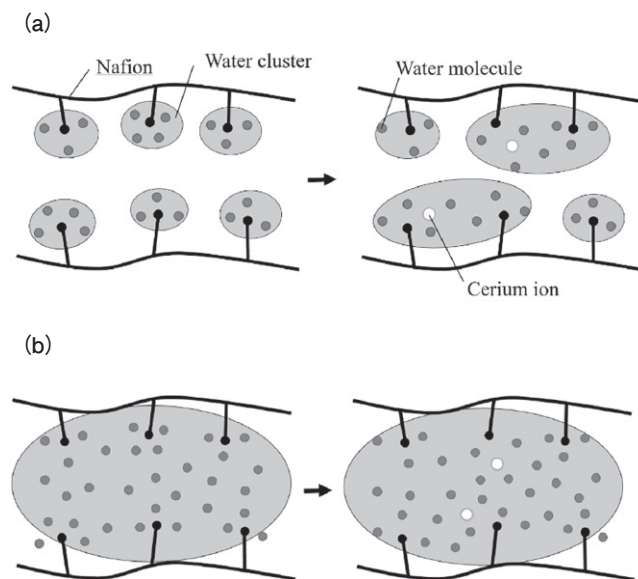
rounding water molecules and the clusters are connected. Hence, the proton diffusion pathways were improved. At the water content of 3 and CAR = 5, 10%, although the proton number density decreases and the membrane resistance increases with the increase CAR, the change is significantly small because the diffusion coefficient of proton increased.

At high water content, the diffusion coefficient of protons decreased due to the addition of cerium ions because water clusters are already well connected, and cerium ions have negligible effect on the cluster structure. In this case, the positive charge of the cerium ion repels the protons and prevents proton diffusion, resulting the increase in the membrane resistance.

The diffusion coefficient of cerium ions increases with increasing water content because the water molecules gathering around the sulfonic acid group shield the charge as the water content increases and the cerium ions diffuse into the water cluster and move freely.

References

1) NEDO: Fuel cell / hydrogen technology development roadmap Detailed version（Fuel cell field）,（2017）.

2) D. D. Borges, G. Gebel, A. A. Franco, et al.: Morphology of supported polymer electrolyte ultrathin films: A numerical study, *J. Phys. Chem. C*, **119**, 1201-1216,（2015）.

3) T. Mabuchi and T. Tokumasu: Effects of water nanochannel diameter on proton transport in proton-exchange membranes, *J. Polym. Sci. Part B Polym. Phys.*, **57**, 867-878,（2019）.

4) T. Mabuchi and T. Tokumasu: Relationship between Proton Transport and Morphology of Perfluorosulfonic Acid Membranes: A Reactive Molecular Dynamics Approach, *J. Phys. Chem. B*, **122**, 5922-5932,（2018）.

5) H. L. Yeager and A. Steck: Cation and water diffusion in nafion ion exchange membranes: Influence of polymer structure, *J. Electrochem. Soc.*, **128**, 1880-1884,（1981）.

6) T. Mabuchi and T. Tokumasu: Dependence of electroosmosis on polymer structure in proton exchange membranes, *Mech. Eng. J.*, **4**, 17-00054-17-00054,（2017）.

7) M. P. Rodgers, L. J. Bonville, H. R. Kunz, et al.: Fuel cell perfluorinated sulfonic acid membrane degradation correlating accelerated stress testing and lifetime, *Chem. Rev.*, **112**, 6075-6103,（2012）.

8) C. Lim, L. Ghassemzadeh, F. Van Hove, et al.: Membrane degradation during combined chemical and mechanical accelerated stress testing of polymer electrolyte fuel cells, *J. Power Sources*, **257**, 102-110,（2014）.

9) M. Inaba, T. Kinumoto, M. Kiriake, et al.: Gas crossover and membrane degradation in polymer electrolyte fuel cells, *Electrochim. Acta*, **51**, 5746-5753,（2006）.

10) J. Healy, C. Hayden, T. Xie, et al.: Aspects of the chemical degradation of PFSA ionomers used in PEM fuel cellsx, *Fuel Cells*, **5**, 302-308,（2005）.

11) L. Gubler, S. M. Dockheer and W. H. Koppenol: Radical（HO·, H· and HOO·）Formation and ionomer degradation in polymer electrolyte fuel cells, *J. Electrochem. Soc.*, **158**,（2011）.

12) E. Endoh: Development of highly durable PFSA membrane and MEA for PEMFC under high temperature and low humidity conditions, *ECS Trans.*, **16**, 1229-1240,（2008）.

13) P. Trogadas, J. Parrondo and V. Ramani: Degradation Mitigation in Polymer Electrolyte Membranes Using Cerium Oxide as a Regenerative Free-Radical Scavenger, *Electrochem. Solid-State Lett.*, **11**, B113,（2008）.

14) E. Endoh, N. Onoda, Y. Kaneko, et al.: Membrane Degradation Mitigation of PEFC during Cold-Start Application of the Radical Quencher Ce^{3+-}, *ECS Electrochem. Lett.*, **2**, F73-F75,（2013）.

15) Current status and issues of FCV fuel cells, *NEDO Issue Shar. Forum*.

16) A. M. Baker, D. Torraco, E. J. Judge, et al.: Cerium migration during PEM fuel cell assembly and operation, *ECS Trans.*, **69**, 1009-1015,（2015）.

17) K. Kawai, T. Mabuchi and T. Tokumasu: Molecular Dynamics Analysis of Proton Diffusivity in Hydrated Nafion Membranes Contaminated with Ferrous Ions, *Macromol. Theory Simulations*, **1900047**, 1-8,（2019）.

18) K. H. Wong and E. Kjeang: In-Situ Modeling of Chemical Membrane Degradation and Mitigation in Ceria-Supported Fuel Cells, *J. Electrochem. Soc.*, **164**, F1179-F1186,（2017）.

19) T. Mabuchi and T. Tokumasu: Effect of bound state of water on hydronium ion mobility in hydrated Nafion using molecular dynamics simulations, *J. Chem. Phys.*, **141**,（2014）.

20) U. Essmann, L. Perera, M. L. Berkowitz, et al.: A smooth particle mesh Ewald method, *J. Chem. Phys.*, **103**, 8577-8593,（1995）.

21) T. Mabuchi, A. Fukushima and T. Tokumasu: A modified two-state empirical valence bond model for proton transport in aqueous solutions, *J. Chem. Phys.*, **143**,（2015）.

22) S. Ochi, O. Kamishima, J. Mizusaki, et al.: Investigation of proton diffusion in Nafion®117 membrane by electrical conductivity and NMR, *Solid State Ionics*, **180**, 580-584,（2009）.

23) W. G. Hoover: Constant-pressure equations of motion, *Phys. Rev. A*, **34**, 2499-2500,（1986）.

24) H. C. Andersen: Molecular dynamics simulations

at constant pressure and/or temperature, *J. Chem. Phys.*, **72**, 2384-2393, (1980).

25）K. H. Wong and E. Kjeang: Simulation of Performance Tradeoffs in Ceria Supported Polymer Electrolyte Fuel Cells, *J. Electrochem. Soc.*, **166**, F128-F136, (2019).

26）S. Kumaraguru: Durable High Power Membrane Electrode Assembly with Low Pt Loading, *Energy.gov Hydrog. Fuel Cells Progr. Annu. Merit Rev.*, **1**, 1-9, (2018).